

RF Single Electron Transistor Readout Amplifiers for Superconducting Astronomical Detectors of X-ray to sub-mm Wavelengths

Thomas R. Stevenson, Abdelhanin Aassime, Per Delsing, Robert Schoelkopf, Ken Segall, and Carl M. Stahle

Abstract We have made Radio-Frequency Single-Electron Transistors (RF-SETs) with large input gates, and tested performance and modes of operation with the goal of using such devices as on-chip amplifiers for a variety of high impedance cryogenic photodetectors. We achieved ≈ 100 kHz of closed-loop bandwidth for charge-locked-loop and transimpedance amplifier feedback configurations, and have combined amplifier outputs using a form of wavelength division multiplexing. With our choice of SET junction resistance, a 0.5 fF input gate capacitance gave a cotunneling-degraded charge noise of $1 \times 10^{-4} e/\sqrt{\text{Hz}}$, but a fairly low input voltage noise of 30 nV/ $\sqrt{\text{Hz}}$.

Index Terms Amplifiers, Feedback, Multiplexing, Photodetectors, Tunneling.

INTRODUCTION

SEVERAL types of superconducting photodetectors are being developed for astronomical applications. Examples include the Transition Edge Sensor (TES) [1], Superconducting Tunnel Junction (STJ) [2], and Single Quasiparticle Photon Counter (SQPC) [3]. Despite the complexity of cryogenic operation, such detectors are desirable because of capabilities such as single-photon spectroscopy, or extreme levels of sensitivity, which cannot be obtained with uncooled detectors.

However, output impedances and levels make low-noise, high-speed readouts challenging, and large format detector arrays require integration with sensitive, fast, compact, low-power, multiplexable, on-chip amplifiers. For high impedance detectors such as the STJ and SQPC, the Radio-Frequency Single-Electron Transistor (RF-SET) [4] seems to be an ideal amplifier.

Single Electron Transistors (SETs) are cryogenic quantum-effect devices which utilize quantization of charge on a small conducting island to yield a very high performance

electrometer [5]. With picowatt power dissipation and sub-femtofarad input capacitance, SETs are well-suited as on-chip amplifiers for detectors with high resistance and low capacitance. With an rf readout technique, the RF-SET increases the readout bandwidth of the SET greatly, to over 100 MHz. In this paper, we describe work on applying RF-SETs to meet the requirements of multi-channel photodetector array readout.

BASIC OPERATION OF THE RF-SET

SETs are electrostatic duals [6] of the better known SQUIDS, which are the most sensitive magnetometers and current amplifiers [7]. When an input voltage V_i is applied to the SET input gate of capacitance C_g , the I - V characteristic seen between source and drain is a periodic function of induced gate charge $\delta Q_g = V_i C_g$ with a period of e , the electronic charge. In an RF-SET, an SET is connected in parallel with a capacitor and in series with an inductor to form a high-frequency (GHz) tank circuit with dissipation modulated by gate charge. An rf carrier signal is applied at the resonance frequency, and the amount of reflected power is measured by a HEMT amplifier [8]. This technique gives sensitive charge measurements while avoiding bandwidth limits caused by cable capacitance and SET output impedance. Bandwidths are as large as 100 MHz, and charge noise $\approx 10^{-5} e/\sqrt{\text{Hz}}$ has been obtained [4].

DETECTOR READOUT SYSTEM DESIGN

Our work on an RF-SET readout system for an array of photodetectors addresses a number of requirements beyond what is necessary to make a fast and sensitive electrometer.

A. Large Input Gate

An STJ detector, for example, converts a photon into a current pulse with a total charge proportional to the photon energy, which, with appropriate detector designs, can range from x-ray [9] to optical [10]. When the detector is connected to the input gate of an RF-SET, the signal charge will be divided between C_g and the detector capacitance plus any stray capacitance. While the RF-SET has an advantage over an FET amplifier in that C_g is small compared to the detector and stray capacitance, C_g should not be chosen any smaller than required to obtain the best SET charge noise Q_n , for then the increasing SET voltage noise Q_n/C_g starts to limit detection sensitivity.

Manuscript received September 19, 2000. This work was supported by internal GSFC Director's discretionary funds, NASA Explorer grant NAG5-8589, the NASA Cross Enterprise Technology Development Program, and equipment funds from the Jet Propulsion Laboratory.

T. R. Stevenson and C. M. Stahle are with Goddard Space Flight Center, NASA/GSFC, Code 553, Greenbelt, MD 20771 USA (e-mail: thomass@pop500.gsfc.nasa.gov). T. R. Stevenson is an employee of Orbital Sciences Corporation.

A. Aassime and P. Delsing are with Chalmers University of Technology, Department of Microelectronics and Nanoscience, Fysikgränd 3, S-41296 Göteborg, Sweden.

R. Schoelkopf and K. Segall are with the Department of Applied Physics, Yale University, PO Box 208284, New Haven, CT 06520-8284 USA.

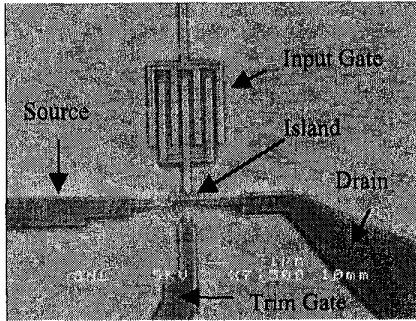


Fig. 1. Scanning electron micrograph of an SET device showing geometry of the finger capacitor design used to obtain a gate capacitance of 0.5 fF. Fingers are 3.0 μm long, 0.25 μm wide, and separated by 0.20 μm .

For our devices, we chose $C_g \approx 0.5$ fF, which then gives about a 50% contribution to the total SET island capacitance $C_x = 2C_J + C_g$, where C_J is the capacitance of one SET junction. For larger values of C_g , the decrease of the Coulomb blockade energy $E_c = e^2/2C_x$ degrades the voltage modulation of the SET and lowers its required operation temperature. We implemented our input gates with the interdigitated structure shown in Fig. 1.

B. Wavelength Division Multiplexing

Another important requirement of the readout system is the capability to multiplex amplifier channels. Below we describe the first demonstration of Wavelength Division Multiplexing (WDM) of RF-SETs.

Our multiplexing concept (Fig. 2) is to connect the tank circuits for many (≈ 30) RF-SETs in parallel to one coaxial cable leading to one HEMT amplifier. Each tank circuit has a unique resonance frequency, and instead of a single frequency carrier wave, a frequency comb is generated with a frequency component corresponding to each resonance. The reflected power signal from each RF-SET amplifier channel can be decoded and demodulated with room temperature rf electronics after amplification by the one cryogenic HEMT amplifier. Simultaneous readout of all the channels is possible.

C. Feedback Modes

Feedback is required to linearize the response of each RF-SET. One mode of applying feedback is to use a small trim gate (see Fig. 1) on each SET to apply a compensating charge which cancels response to an input gate signal. We call that mode of operation a Charge-Locked-Loop (CLL) in analogy with the flux-locked-loop operation of dc SQUIDs [7].

However, for continuous detection of a photocurrent, the charge must be drained away to maintain an appropriate bias voltage on the detector. This can be done by canceling the photocurrent at the input gate by supplying a feedback current through a (cold, on-chip) resistance R_{fb} (Fig. 2). In this second mode of operation, the RF-SET acts as a transimpedance amplifier, with an output voltage equal to $-R_{fb}$ times the photocurrent. A voltage on the trim gate can be used to adjust the operating voltage bias on the detector.

We have operated our RF-SET amplifiers in both these modes of closed-loop operation.

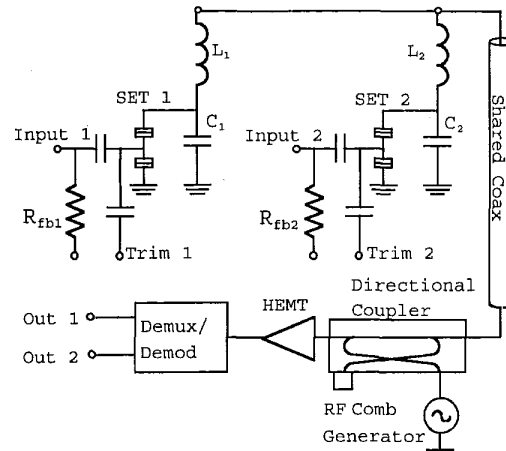


Fig. 2. Schematic circuit showing WDM multiplexing scheme (for two channels) and terminals for input, output, and feedback. All tank circuit inductors are connected to a shared coaxial cable running from the subkelvin detector chip to components at 4 K. Multiple carrier frequencies pass through the directional coupler to excite each tank circuit. Reflected power is directed to the input of the HEMT amplifier. Outputs are demultiplexed and demodulated at room temperature, and feedback to trim gates (feedback resistors) for CLL (transimpedance) modes of closed-loop operation.

FABRICATION

Our SETs were fabricated with aluminum thin films on oxidized silicon chips using a JEOL e-beam lithography system and a standard double-angle evaporation technique [11] in the Swedish Nanometer Laboratory at Chalmers University of Technology.

The tunnel junctions of the SET had an overlap area of about 60 nm \times 60 nm. The combined resistance of the two junctions was varied from about 30 k Ω to 200 k Ω by changing the pressure or time during oxidation to form the tunnel barriers.

We made our rf tank circuits using small chip inductors wire bonded to the input gate pad and a SMA microstrip launcher. Inductance values were near 200 nH, and the ≈ 0.5 pF tank capacitance consisted of pad capacitances to ground.

MEASUREMENTS OF THE SET CHARACTERISTICS

We cooled our devices down to 250 mK in a ^3He refrigerator. Cryogenic powder filters [12] provided high frequency filtering and heatsinking of all SET connections except the rf input/output coax, which had an attenuator at 4K and a directional coupler to reduce thermal radiation reaching the SET.

Most of our measurements were made with the aluminum SETs in the superconducting state, since applying a high magnetic field will not be possible when integrated with STJ or SQPC detectors.

To measure I - V characteristics, we used a bias-tee located on the cold stage to apply both dc and rf bias. We applied a dc bias current through a room temperature bias resistor, typically 100 k Ω , and measured dc voltages across the SET and bias resistor with room temperature electronics.

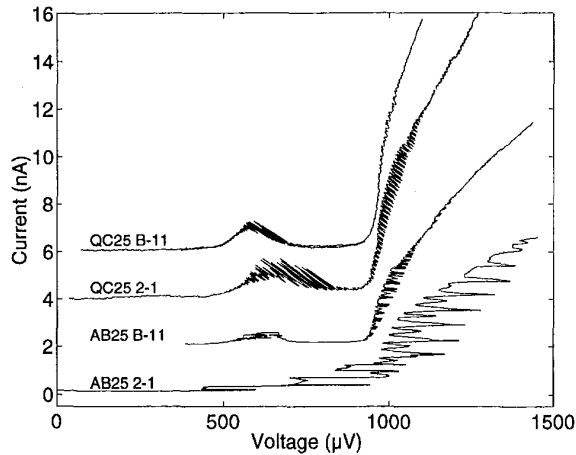


Fig. 3. I - V characteristics of the SET devices with an oscillating gate signal applied. Curves are offset vertically by 2 nA from each other.

Fig. 3 shows I - V curves for several devices measured with no rf carrier applied, but with a several-electron oscillating gate charge signal applied to the input or trim gate. Modulation is seen in Fig. 3 both above the Giaever gap rise, and on the JQP peak in the subgap region [13]. We also observed supercurrent modulation [14] with amplitude as large as 20 pA peak-to-peak near zero bias.

Device parameters measured from the I - V data are listed in Table I. One pair of devices on the same chip had a sum of junction resistances $R_n = R_1 + R_2 \approx 64$ k Ω , while a pair on another chip had $R_n \approx 110$ k Ω . In each pair, one device had a large input gate, and one did not. The junction size in each pair were similar, but the higher resistance pair had smaller junctions. The spacing of modulation nodes in the superconducting state, or the offset voltage in the normal state for QC25 B-11, were used to determine C_Σ . The periodicity of gate coupling gave C_g . The location of the Giaever current rise and the temperature dependence of the subgap current gave consistent values for the superconducting gap Δ .

TABLE I
SET DEVICE PARAMETERS

Device	R_n	C_Σ	C_g	Δ/e	α
QC25 B-11	64.1 k Ω	1.30 fF	0.56 fF	237 μ V	3.1
QC25 2-1	63.9	0.74	-	237	1.8
AB25 B-11	108.7	0.84	0.53	234	1.2
AB25 2-1	105.9	0.32	-	234	0.46

As seen in Fig. 3, the large gate devices showed much poorer modulation above the gap than small gate devices, and larger resistance devices worked better than those with low resistance. Large gate devices with $R_n = 30$ k Ω did not show any detectable modulation.

We understood this behavior in the context of the cotunneling theory of Averin *et al.* [15]. Their parameter α , defined by

$$\alpha = \Delta/E_c \cdot h/e^2 (1/R_1 + 1/R_2)/2,$$

determines the threshold at which the energy width of the island charge states, set by the I/e frequency, will equal the Coulomb blockade energy. For $\alpha < 1$, the blocked conductance scales as α^2 , while for $\alpha > 1$, rapid cotunneling causes the modulation to vanish rapidly.

Initially, we focussed on making low resistance SETs with the goals of larger absolute current modulation and better rf coupling. Faced with the very poor above-gap modulation of device QC25 B-11, for example, we found we could choose a combination of dc and rf bias to operate the RF-SET on its JQP peak instead. We then measured an open-loop charge noise of $1 \times 10^{-4} e/\sqrt{\text{Hz}}$ above a $1/f$ -knee at 2 kHz. The white noise was limited by the HEMT amplifier noise and the suboptimal SET modulation. A very similar noise level was obtained with the later device AB25 B-11 operating on the gap rise. With the 0.5 fF input gate capacitance, the charge noise was equivalent to a voltage noise of 30 nV/ $\sqrt{\text{Hz}}$.

DEMONSTRATION OF WDM

By wirebonding two chip inductors to a pair of SETs on the same chip, we investigated the rf multiplexing scheme using two channels. The rf power reflected from the parallel combination of the two tank circuits is shown versus frequency in Fig. 4. By appropriate selection of inductances, resonances at 392 and 497 MHz were separated by about twice their individual width.

Fig. 4 also shows in the time domain the demultiplexed outputs of the two RF-SETs responding to different gate charge triangle-wave signals. The open-loop response to the ramping gate signals was approximately sinusoidal for each RF-SET. With Fourier analysis of the Fig. 4 data, we found an 8% coupling of Ch. 2 in the Ch. 1 output, and 4% of Ch. 1 in Ch. 2. This cross-coupling effect, where impedance changes of one SET off-resonance perturb the reflection of the carrier allocated for a different SET, will be diminished when feedback is used to fix each SET's operating point. The closed-loop coupling will then depend on the cross-capacitance between gates, which we can reduce by adding appropriate grounded guard traces in our e-beam layout.

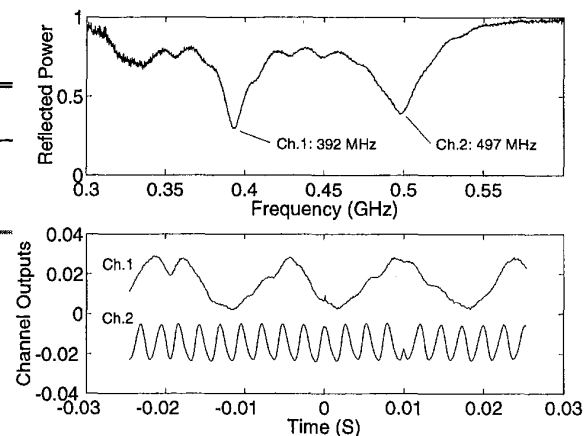


Fig. 4. Two-channel demonstration of wavelength division multiplexing. At top, the ratio of the reflected power with the SET in a high/low impedance state is shown versus frequency. The resonance frequencies are 392 and 497 MHz. Demultiplexed signals (below) show little cross-talk.

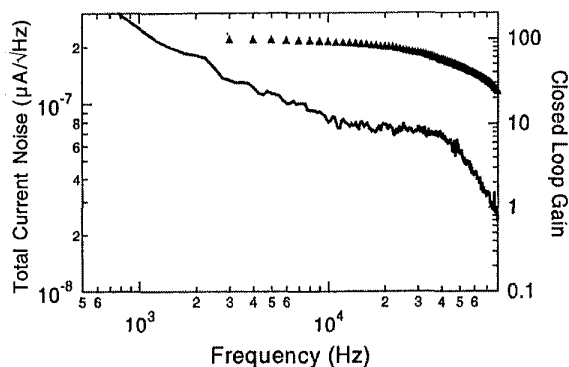


Fig. 5. Closed loop noise spectrum and gain for an RF-SET operated as a transimpedance amplifier.

CLOSED-LOOP RESPONSE

We tested both the CLL and transimpedance modes of closed-loop operation, described above. We found that forming a stable CLL with up to 100 kHz of bandwidth was relatively easy, and that, we could maintain the $1 \times 10^{-4} e/\sqrt{\text{Hz}}$ white noise level seen open-loop.

To form a transimpedance amplifier, we wirebonded the input gate pad to a set of three 1 M Ω chip resistors, which served as the feedback resistor, a dummy load to simulate a high impedance photodetector, and a port for injecting a simulated photocurrent.

Achieving a stable transimpedance amplifier loop was more challenging than the CLL because of the RC time constant seen at the input gate terminal, as well as other additional time constants in the room temperature part of the feedback loop. Compromising on SET gain a bit with a non-optimal operating point, we achieved a stable loop with ≈ 50 kHz of bandwidth (see Fig. 5). In the white noise region, we measured a total equivalent input current noise of about 85 fA/ $\sqrt{\text{Hz}}$, as expected from the sum of the three load and feedback conductances multiplied by the 30 nV/ $\sqrt{\text{Hz}}$ voltage noise of the RF-SET we observed open loop.

CONCLUDING REMARKS

We have investigated the performance of RF-SETs with large input gates as potential on-chip amplifiers for high impedance superconducting photodetectors, and we have made a successful first demonstration of a wavelength division multiplexing scheme for these amplifiers.

We identified minimizing cotunneling as an important SET design requirement for optimizing the readout amplifier gain and noise. While our multiplexing demonstration was done using discrete chip inductors, we have recently made lithographic inductors less than 1 mm in diameter on substrate chips for miniaturization and integration with SETs. Our goal is about 30 WDM channels per coax.

The voltage noise level we achieved for transimpedance amplifier operation, while far from optimal, would be sufficient to readout a 5000 A/W responsivity SQPC submillimeter detector with a noise equivalent power NEP $\approx 10^{-18}$ W/ $\sqrt{\text{Hz}}$. Ultimate sensitivities of 10^{-20} W/ $\sqrt{\text{Hz}}$ are projected [3].

ACKNOWLEDGMENT

We thank Peter Walgren for early device fabrication for us at Chalmers University, and Daniel Prober, Luigi Frunzio, and Chris Wilson at Yale University for valuable discussions. We also thank Richard Bradley of the National Radio Astronomy Observatory for supplying the ultralow noise HEMT amplifier, and Irfan Siddiqi, Aleksandr Verevkin, and Shunjiang Xu at Yale University for valuable laboratory assistance.

REFERENCES

- [1] K. D. Irwin, G.C. Hilton, D. A. Wollman *et al.*, "Thermal-response time of superconducting transition-edge microcalorimeters" *J. Appl. Phys.* vol. 83, pp. 3978-3985, Apr. 1998; C. K. Stahle, R. P. Brekosky, E. Figueroa-Feliciano, *et al.*, "Progress in the development of Mo/Au transition-edge sensors for x-ray spectroscopy," *Proc. SPIE*, vol. 4140, in press.
- [2] N. Rando, S. Andersson, B. Collaudin, *et al.*, "S-Cam: A cryogenic camera for optical astronomy based on superconducting tunnel junctions," *IEEE Trans. Appl. Supercond.*, vol. 10, pp. 1617-1625, Jun. 2000.
- [3] R. J. Schoelkopf, S. H. Moseley, C. M. Stahle, P. Wahlgren, P. Delsing, "A concept for a submillimeter-wave single-photon counter," *IEEE Trans. Appl. Supercond.*, vol. 9, pp. 2935-2939, Jun. 1999.
- [4] R. J. Schoelkopf, P. Wahlgren, A. A. Kozhevnikov, P. Delsing, D. E. Prober, "The radio-frequency single-electron transistor (RF-SET): A fast and ultrasensitive electrometer," *Science*, vol. 280, pp. 1238-1242, May 1998; A. Aassime, P. Delsing, R. J. Schoelkopf, "Radio frequency single-electron transistor: towards the quantum limit," *IEEE Trans. Appl. Supercond.*, submitted for publication.
- [5] T. A. Fulton and G. J. Dolan, "Observation of single-electron charging effects in small tunnel-junctions," *Phys. Rev. Lett.*, vol. 59, pp. 109-112, Jul. 1987.
- [6] K. K. Likharev, "Single-electron transistors — electrostatic analogs of the dc SQUIDS," *IEEE Trans. Magn.*, vol. 23, pp. 1142-1145, Mar. 1987.
- [7] J. Clarke, "Principals and applications of SQUIDS," *Proc. IEEE*, vol. 77, pp. 1208-1223, Aug. 1989.
- [8] Our HEMT amplifier was provided by the National Radio Astronomy Observatory, 2015 Ivy Road, Suite 219, Charlottesville, VA 22903.
- [9] L. Li, L. Frunzio, K. Segall, *et al.*, "Single-photon 2-D imaging X-ray spectrometer employing trapping with four tunnel junctions," *Nucl. Instr. Meth. Phys. Res. Sec. A*, vol. 444, pp. 228-231, Apr. 2000.
- [10] C. M. Wilson, K. Segall, L. Frunzio, *et al.*, "Optical/UV single-photon imaging spectrometers using superconducting tunnel junctions," *Nucl. Instr. Meth. Phys. Res. Sec. A*, vol. 444, pp. 449-452, Apr. 2000.
- [11] G. J. Dolan, "Offset masks for lift-off processing," *Appl. Phys. Lett.*, vol. 31, pp. 337-339, 1977.
- [12] A. Fukushima, A. Sato, A. Iwasa, *et al.*, "Attenuation of microwave filters for single-electron tunneling experiments," *IEEE Trans. Instr. Meas.*, vol. 46, pp. 289-293, Apr. 1997.
- [13] T. A. Fulton, P. L. Gammel, D. J. Bishop, L. N. Dunkleberger, and G. J. Dolan, "Observation of combined Josephson and charging effects in small tunnel junction circuits," *Phys. Rev. Lett.*, vol. 63, pp. 1307-1310, Sep. 1989.
- [14] A. Amar, D. Song, C. J. Lobb, F. C. Wellstood, "Superconducting Coulomb-blockade electrometers with tunable Josephson coupling," *IEEE Trans. Appl. Supercond.*, vol. 7, pp. 3544-3547, Jun. 1997.
- [15] D. V. Averin, A. N. Korotkov, A. J. Manninen, J. P. Pekola, "Resonant tunneling through a macroscopic charge state in a superconducting single electron transistor," *Phys. Rev. Lett.*, vol. 78, pp. 4821-4824, Jun. 1997.